4. B. W. Kim and J. H. Choy, *Bull. Kor. Chem. Soc.*, in press (1988).
5. C. Michel and B. Raveau, *J. Solid State Chem.*,**43**, 73 (1982).
6. K. Kojima, K. Ohbayashi, M. Udagawa, and T. Hihara, *Jpn. J. Appl. Phys.*, **26**, L766 (1987).
7. J. H. Choy, S. H. Byeon, S. T. Hong, D. Y. Jung, S. Y. Choy, B. W. Kim, J. T. Kim, D. Y. Noh, H. I. Yoo, D. N. Lee, D. Y. Seung, T. S. Park, *J. Kor. Cer. Soc.*,**25** , 154 (1988).
8. A. R. Rossi and R. Hoffmann, *Inorg. Chem.*, **14**, 365 (1975).
9. D. E. Billing, R. J. Dudley, B. J. Hathaway, and A. A. G. Tomlinson, *J. Chem. Soc. (A)*, 691 (1971).
10. R. J. Dudley, B. J. Hathaway, P. G. Hodgson, P. C. Power, and D. J. Loose, *J. C. S. Dalton*, 1005 (1974).
11. B. J. Hathaway, *J.C.S. Dalton*, 1196 (1972).
12. A. B. P. Lever, *"Inorganic Electronic Spectroscopy"* Elsevier, p.568 (1984).
13. M. F. Yan, R. L. Barns, H. M. O'Bryan, Jr., P. K. Gallagher, R. C. Sherwood, and S. Jin, *Appl. Phys. Lett.***51**, 532 (1987).
14. B. G. Hyde, J. G. Thompson, R. L. Withers, J. G. Fitz-Gerald, A. M. Stewart, D. J. Bevan, J. S. Anderson, J. Bitmead, and M. S. Paterson, *Nature*, **327**, 402 (1987).
15. A. Barkatt, H. Hojaji, and K. A. Michael, *Adv. Ceramic Mater.*, **2**, No. 3B, 701 (1987).
16. J. H. Choy, S. H. Chun, B. W. Kim, D. Y. Jung, S. T. Hong, and S. H. Byeon, *Bull. Kor. Chem. Soc.*, **9**, 240 (1988).
17. Y. Kitano, K. Kifune, I. Mukouda, H. Kamimura, J. Sakurai, Y. Komura, K. Hoshino, M. Suzuki, A. Minami, Y. Maeno, M. Kato, and T. Fujita, *Jpn. J. Appl. Phys.*, **26**, L394 (1987).

# Preparation, Structural and Magnetic Properties of Ordered Perovskite (BaLa)(MgMo)$O_6$

**Jin-Ho Choy* and Seung-Tae Hong**

*Department of Chemistry, Seoul National University, Seoul 151-542*
*Received June 3, 1988*

The polycrystalline powder of (BaLa)(MgMo)$O_6$ has been prepared at 1350 °C in a nitrogen flowing atmosphere. The powder X-ray diffraction pattern indicates that (BaLa)(MgMo)$O_6$ has a cubic perovskite structure ($a_o$ = 8.019(3) Å) with 1 : 1 ordering or $Mg^{2+}$ and $Mo^{5+}$ in the oxide lattice. The infrared spectrum shows two strong absorption bands with their maxima at 600($\nu_3$) and 365 ($\nu_4$) $cm^{-1}$, which are attributed to $2T_{1U}$ modes of molybdenum octahedra $MoO_6$ in the crystal lattice. According to the magnetic susceptibility measurement, the compound shows a paramagnetic behavior which follows the Curie-Weiss law below room temperature with the effective magnetic moment 1.60(1) $\mu_B$, which is consistent with that of spin only value (1.73 $\mu_B$) for $Mo^{5+}$ ($4d^1$ electronic configuration). From the thermogravimetric and X-ray diffraction analyses, it has been found that (BaLa)(MgMo)$O_6$ decomposes gradually into $BaMoO_4$, $MoO_3$ and unidentified phases above 900 °C in an ambient atmosphere, absorbing about 0.25 mole $O_2$ per mole of Mo ion, which also supports that oxidation state of $Mo^{5+}$ in the (BaLa)(MgMo)$O_6$.

## Introduction

In perovskite type compounds as $A_2(BB')O_6$ and (AA')(BB')$O_6$, the A and A' cations are coordinated with twelve oxygen ions and B and B' cations with six. It is well known that an ordered distribution of B and B' ions along (111) planes is most probable when a large difference exists in either their charges or ionic radii.[1] Figure 1 shows the arrangement of ions in the (100) plane of the cubic perovskite lattice for (AA')(BB')$O_6$ type compounds, where B and B' cations are alternatively arranged between oxygen ions. Holes denoted by * in Figure 1 are randomyl occupied by A and A' cations. In the ordered structure oxygen atoms are slightly shifted toward the more highly charged cation, but the octahedral symmetry of the B and B' cations is retained. Many compounds are known to have such an ordered structure on the octahedral sublattice (B-site), while few compounds[2] have been found to have a crystallographic ordered structure on the twelve-coordinated cation sublattice (A-site).

Sleight and Weiher[3] reported the valency pairs (M,Re) (M = Mn,Fe,Co and Ni) in the ordered perovskites $Ba_2(MRe)O_6$, where they confirmed the valency state from the structural point of view rather than from physical characterizations.

When A cation is divalent and A' trivalent in (AA')(BB')$O_6$, the valency pair (B,B') should be one of three possible pairs (1+,6+), (2+,5+) and (3+,4+) by the charge neutrality condition.

The ordered perovskite structure were reported for all the compounds with the formula of (CaLa)(B(II)B(V))$O_6$, where (B(II), B'(V)) = ($Mg^{2+}$, $Mo^{5+}$)[4], ($Mg^{2+}$, $Ru^{5+}$), ($Mg^{2+}$, $Ir^{5+}$), ($Ca^{2+}$, $Ta^{5+}$), ($Mn^{2+}$, $Mo^{5+}$) and ($Mn^{2+}$, $Ta^{5+}$), while random distribution was observed for the valency pair (B(III), B'(IV)) = ($Mn^{3+}$, $Ti^{4+}$).[5-7]

In the present study an attention was paid to the formation of ordered valency pair of ($Mg^{2+}$, $Mo^{5+}$) in the complex

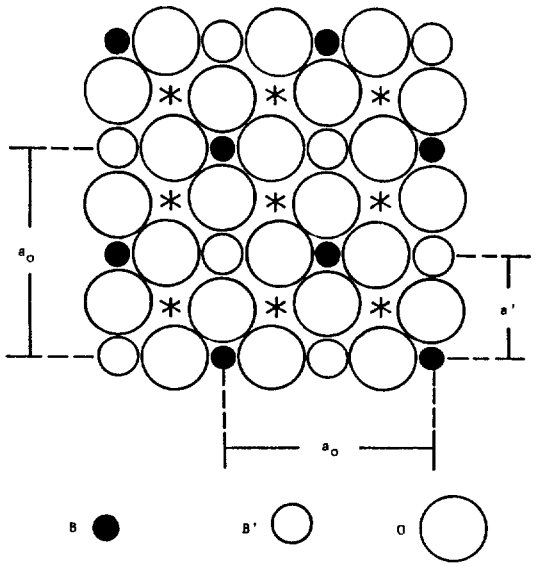


**Figure 1.** Rocksalt arrangement of B and B′ cations in the (100) plane of the cubic perovskite structure for (AA′)(BB′)$O_6$. The Lattice constant $a_o$ and the dimension of one perovskit sub unit a′ are shown.

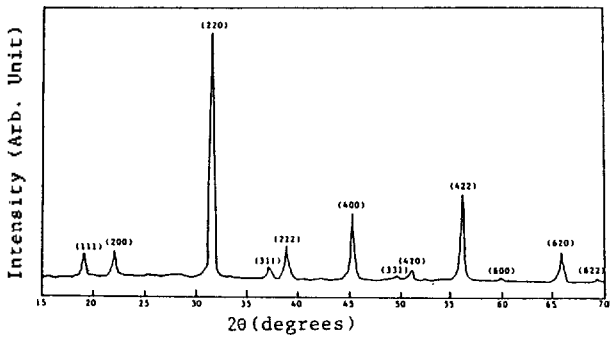


**Figure 2.** Powder X-ray diffraction pattern for (BaLa)(MgMo)$O_6$.

perovskite (BaLa)(MgMo)$O_6$, where the most basic $Ba^{2+}$ ion among alkali earth metal ones is stabilized in the twelve coordinated sites, and to its physico-chemical characterization by X-ray diffraction, infrared spectroscopic, thermogravimetric and magnetic susceptibility measurements.

## Experimental

The polycrystalline powder of (BaLa)(MgMo)$O_6$ was prepared by thermal decomposition of $Ba(NO_3)_2$, $La(NO_3)_3 \cdot 6H_2O$, $Mg(NO_3)_2 \cdot 6H_2O$ and $MoO_3$. The stoichiometric mixture of corresponding nitrates was dissolved in water and heated it to corresponding oxides. The oxide mixture was pressed into pellet and heated in alumina boat at 1350 °C for several hours under a nitrogen flowing atmosphere. The above process was repeated until a homogeneous product was obtained.

The resultant phases and lattice constant of the reaction product were determined by a powder X-ray diffraction method with nickel-filtered Cu-K$\alpha$ (wavelength = 1.5418 Å), using a Jeol X-ray diffractometer.

Infrared absorption spectrum was obtained in the wavenumber range from 200 $cm^{-1}$ to 3000 $cm^{-1}$, using a CsBr pellet with a Jasco Diffraction grating Infrared Spectrophotometer.

Magnetic susceptibilities were measured with a Faraday-type magnetobalance in the temperature range from 77 to 300 K.

Thermogravimetric analysis was carried out from room temp. to 727 K under an ambient atmosphere with a Rigaku Thermal Analysis Station Tas 100.

**Table 1. Powder X-ray Diffraction Data for (BaLa)(MgMo)$O_6$**

| h k l | dobs. (A) | dcal. (A) | Iobs. | Ical. (I) | Ical. (II) |
|---|---|---|---|---|---|
| 1 1 1 | 4.634 | 4.630 | 9.2 | 9.75 | 0.01 |
| 2 0 0 | 4.011 | 4.010 | 11.3 | 10.99 | 10.99 |
| 2 2 0 | 2.835 | 2.835 | 100.0 | 100.00 | 100.00 |
| 3 1 1 | 2.416 | 2.418 | 4.8 | 5.11 | 0.01 |
| 2 2 2 | 2.314 | 2.315 | 15.0 | 17.14 | 17.14 |
| 4 0 0 | 2.005 | 2.005 | 30.5 | 33.21 | 33.21 |
| 3 3 1 | 1.839 | 1.840 | 3.6 | 2.21 | 0.00 |
| 4 2 0 | 1.793 | 1.793 | 5.4 | 5.79 | 5.79 |
| 4 2 2 | 1.636 | 1.637 | 38.0 | 38.69 | 38.69 |
| 3 3 3 / 5 1 1 | 1.544 | 1.543 | 2.3 | 0.41 / 1.22 | 0.00 / 0.00 |
| 4 4 0 | 1.416 | 1.418 | 16.3 | 19.47 | 19.47 |
| 5 3 1 | 1.356 | 1.356 | 1.3 | 1.54 | 0.00 |
| 6 0 0 | 1.337 | 1.337 | 2.9 | 0.60 | 0.60 |
| 6 2 0 | 1.267 | 1.268 | 14.6 | 16.73 | 16.73 |
| 6 2 2 | 1.209 | 1.209 | 2.5 | 4.98 | 4.98 |
| 4 4 4 | 1.157 | 1.157 | 5.4 | 6.53 | 6.53 |
| 6 4 2 | 1.071 | 1.072 | 16.1 | 21.01 | 21.01 |
| 6 6 0 | 0.9456 | 0.9450 | 10.0 | 4.73 | 4.73 |
| 8 4 0 | 0.8969 | 0.8966 | 9.8 | 14.49 | 14.49 |

The theoretical intensity has been calculated by the computer program written in our laboratory, which is based on the eq. $I = |F|^2 P \left(\frac{1+\cos^2\theta}{\sin^2\theta\cos\theta}\right) e^{-2M}$, (ref. 19). Ical.(I); only $Mg^{2+}$ and $Mo^{5+}$ ions are assumed to be ordered. Ical.(II); only $Ba^{2+}$ and $La^{3+}$ ions are assumed to be ordered.

## Results and Discussion

### 1. Preparation

In the preparation of complex perovskite (BaLa)(MgMo)$O_6$ no single phase could be isolated under an ambient atmosphere. The major phase observed in the X-ray diffraction pattern was $BaMoO_4$ with scheelite structure[8], where $Mo^{6+}$ ion is stabilized in a tetrahedral site as a $MoO_4$ tetrahedron.

In order to stabilize $Mo^{5+}$ in an octahedral site in the perovskite, $Mo^{6+}$ in the starting material of $MoO_3$ had to be reduced to $Mo^{5+}$. The synthesis could be achieved only under the reducing condition, that is, a deoxygenized nitrogen flowing atmosphere.

### 2. Crystallographic Analysis

The X-ray powder diffraction pattern (Figure 2) indicates that (BaLa)(MgMo)$O_6$ has a perovskite structure with superlattice lines (111, 311, 331, 333, 511 and 531) caused by the rock-salt arrangement (1:1 ordering) of $Mg^{2+}$ and $Mo^{5+}$ ions in the BB′-sites of the perovskite lattice (AA′)(BB′)$O_6$. All the diffraction lines are indexed by a face-centered cubic unit cell (lattice constant $a_o$=8.019(3) Å) with doubled edge of the sim-

**Table 2. Lattice Constants and Perovskite Parameter $a = \sqrt[3]{V_p}$ of Perovskite-type Compounds (BaLa)(BB′)$O_6$ used in This Work**

| (BB′) | lattice parameter $a_o$ (Å) | $\bar{a}$ (Å) | remarks | ref. |
|---|---|---|---|---|
| MgMo | 8.019(3) | 4.010 | ($Mg^{2+}$,$Mo^{5+}$) ordered | this work. |
| MgRu | 7.957 | 3.979 | ($Mg^{2+}$,$Ru^{5+}$) | 10 |
| CoRu | 7.970 | 3.985 | ($Co^{2+}$,$Ru^{5+}$) | 10 |
| NiRu | 7.935 | 3.968 | ($Ni^{2+}$,$Ru^{5+}$) | 10 |
| ZnRu | 7.982 | 3.991 | ($Zn^{2+}$,$Ru^{5+}$) | 10 |
| MnMo | 8.119(2) | 4.060 | ($Mn^{2+}$,$Mo^{5+}$) | 11 |
| MnTa | 8.173(2) | 4.087 | ($Mn^{2+}$,$Ta^{5+}$) | 12 |
| MgTa | 8.057(2) | 4.029 | ($Mg^{2+}$,$Ta^{5+}$) | 12 |
| FeTa | 8.150(2) | 4.075 | ($Fe^{2+}$,$Ta^{5+}$) | 12 |

ple perovskite one.

For a complex perovskite (AA′)(BB′)$O_6$, there can be three types of ordered and one disordered structures: 1) A and A′ are ordered but B and B′ are randomly distributed, 2) B and B′ are ordered with A and A′ disordered, 3) both A and B-site ions are ordered, and 4) both A and B-site are disordered.

The intensities have been calculated according to the above four assumptions, which have revealed that the B-site ions ($Mg^{2+}$ and $Mo^{5+}$) are ordered in the crystal lattice (see Table 1), but it could not be determined from powder XRD intensities whether $Ba^{2+}$ and $La^{3+}$ ions in A-sites are ordered or not because the atomic scattering factors of $Ba^{2+}$ and $La^{3+}$ are almost the same. However, considering that A-site ions are found to be distributed randomly even in the case of (CaLa)(MgMo)$O_6$[4] and (SrLa)(MgMo)$O_6$[9], where atomic scattering factors between two ions in A-site are so different, $Ba^{2+}$ and $La^{3+}$ ions are considered to be distributed at random in the oxygen-cuboctahedral sites. Reliability factor for this calculation was 8.0%.

For all the other compounds reported previously in the literature[10-12] with the formula of (BaLa)(BB′)$O_6$ where (B(II),B′(V)) = (MgRu), (CoRu), (NiRu), (ZnRu), (MnMo), (MnTa), (MgTa) and (FeTa), the superlattice lines caused by an ordered arrangement of B and B′ ions in the oxygen-octahedral sites were also found in the X-ray diffraction patterns (Table 2).

As shown in Fig. 3, the perovskite parameter a (see Table 2) defined as the cube root of cell volume of the perovskite unit, was plotted against the mean ionic radius $\bar{r} = \frac{1}{2}(r_B + r_{B'})$ in order to check whether they follow the linear relationship or not. The ionic radii used in this plot was obtained from the literature by R.D. Shannon.[13] Perhaps it will be a simple and rough measure to predict the ordering of valency pair (BB′) for the first approximation. Figure 3 indicates clearly that all the other Ba compounds with ordered valency pairs of (B(II), B(V)) follow the linear relationship as well as (BaLa)(MgMo)$O_6$. This can also be one evidence indicating the ordered arrangement of Mg and Mo ions due to the relatively large size and charge difference.[1]

### 3. Infrared Spectrum

In order to confirm the local symmetry of highly charged Mo ions which are stabilized in the perovskite lattice, the in-

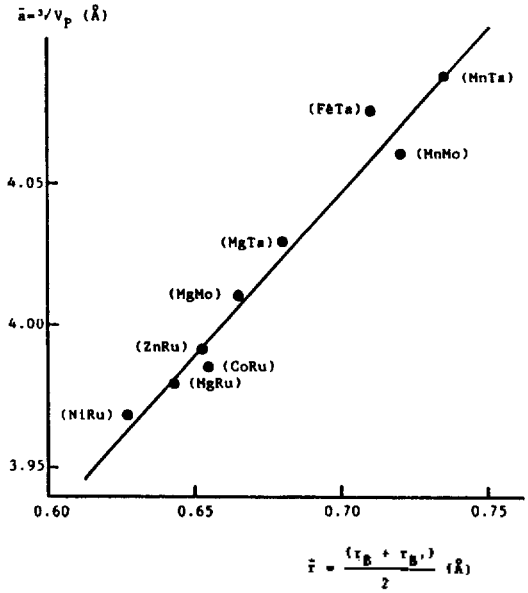


**Figure 3.** The lineare relation between cube root of cell volume versus mean ionic radius of (BB′) ions in perovskites (BaLa)(BB′)$O_6$.

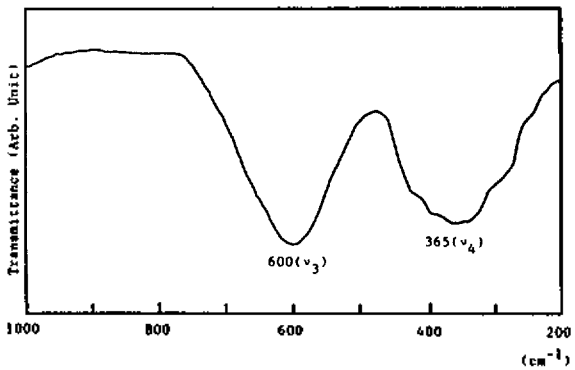


**Figure 4.** IR spectrum for (BaLa)(MgMo)$O_6$.

frared absorption spectrum was obtained, where two strong absorption bands were observed with their maxima at 600 and 365 $cm^{-1}$ as shown in Figure 4.

According to the IR study of ordered perovskites of the type $A_2$(BB′)$O_6$, Blass *et al.*[14,15] reported that the highly charged B ion octahedra like $W^{4+}O_6$, $Mo^{6+}O_6$, $Nb^{5+}O_6$ and $Ti^{4+}O_6$ could act as independent groups and the vibrational spectrum arises from such $BO_6$ octahedra. Assuming that the binding forces between Mo-O in the $MoO_6$ octahedron are large compared with the crystal lattice energy, the frequencies of the internal vibrations of this group in the solid must be close to the frequencies of the free ion modes. Furthermore, the external modes would show lower frequency than the internal modes. Group theoretical considerations represent the normal vibrational modes of an octahedral molecule as

$$A_{1g} + E_g + 2T_{1u} + T_{2g} + T_{2u}$$

Since the two $T_{1u}$ modes are IR-active and there is only one $BO_6$ groups per primitive unit cell, two vibrational absorption bands are expected.

In all cases of $ABO_3$ or $A_2$(BB′)$O_6$ perovskites, normally two strong absorption bands around 600 and 400 $cm^{-1}$ are assigned to $\nu_3$ and $\nu_4$ modes of the octahedra.[14-17] In addition the weak band around 300 $cm^{-1}$ is ascribed to the vibration of

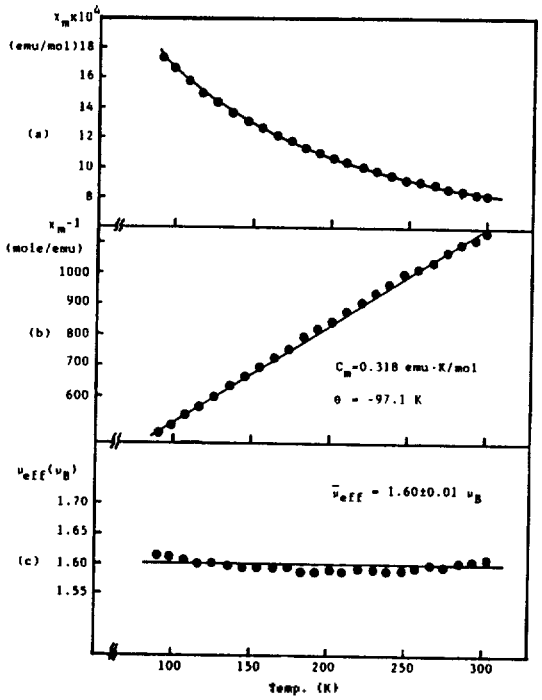


**Figure 5.** Temperature dependence of molar magnetic susceptibility $X_m$ (a), $X_m^{-1}$ (b) and effective magnetic moment $u_{eff}$ (c) of (BaLa)(MgMo)$O_6$.

the $MgO_6$ octahedra rather than the external vibration.

From the IR study, the local symmetry of Mo ion in the oxide lattice (BaLa)(MgMo)$O_6$ is determined to be octahedral, which is well commensurate with the results of the structural analysis.

**4. Magnetic Susceptibility Measurement**

In order to determine the oxidation state of molybdenum ion in the lattice (BaLa)(MgMo)$O_6$, magnetic susceptibility was measured from 77 K to 300 K. Temperature dependence of magnetic susceptibility per a mole of molybdenum ion is shown in Figure 5. Diamagnetic contribution of every ions to $X_m$ was corrected according to Selwood[18]. The $X_m$'s of (BaLa)(MgMo)$O_6$ obeys the Curie-Weiss law below room temperature with the effective magnetic moment per Mo ion of 1.60(1)$\mu_B$. The Curie constant $C_m$ and Weiss constant $\theta$ obtained from the least square fit of $X_m^{-1} = (T-\theta)/C_m$ for all the temperature have been estimated as 0.32 (emu·K/mole) and -97.1 K, respectively.

The observed effective magnetic moment 1.60 $\mu_B$ is consistent with the spin only value of $Mo^{5+}$($4d^1$-state), within the limit of experimental error (~7%). Such a deviation of the magnetic moment (0.13 $\mu_B$) might to due to the effect of the spin-orbit coupling and/or the existence of a trace of $Mo^{6+}$ ion ($4d^0$ electronic configuration).

**5. Thermogravimetric(TG) analysis**

According to the TG analysis of (BaLa)(MgMo)$O_6$ under ambient atmosphere, the oxygen absorption is significant in the temperature range from room temperature to 727 K as shown in Figure 6, where a drastic mass increase is observed in two steps, which might be attributed to the successive oxidation and decomposition reaction as follows:

$$(BaLa)(MgMo)O_6 + (x/4)O_2 \rightarrow \begin{cases} BaLaMgMo^{5+}_{1-x}Mo^{6+}_{x}O_{6+x/2} \\ BaMo^{6+}O_4 + MoO_3 + \text{unidentified phases} \end{cases}$$

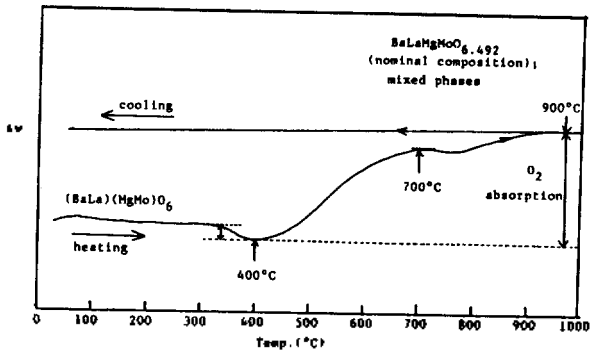


**Figure 6.** Thermogravimetric analysis of (BaLa)(MgMo)$O_6$ under an ambient atmosphere.

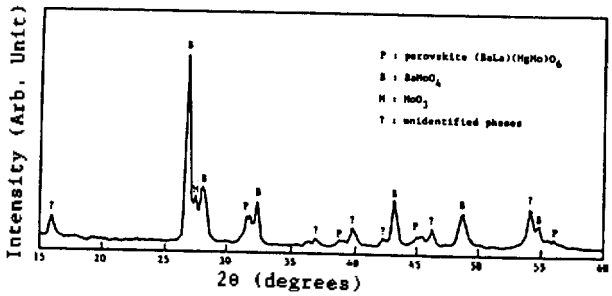


**Figure 7.** Powder X-ray diffraction pattern after oxidative decomposition of (BaLa)(MgMo)$O_6$ (The heat treated sample over 900 °C in TG analysis).

In Figure 6 the slight mass decrease before the point of a drastic mass increase might be ascribed to dehydration and/or decarbonation effects on the surface of the fine particles. The content of oxygen 0.246 mole absorbed per mole of Mo ion in TG analysis, is very close to the calculated value of 0.25 mole when the $Mo^{5+}$ ion are assumed to be oxidized completely to $Mo^{6+}$.

The XRD pattern of the oxidized compound is shown in Figure 7, where original perovskite phase could merely be seen, but $BaMo^{6+}O_4$ could be easily identified as a major phase[8], which indicates also that Mo ion is stabilized in (BaLa)(MgMo)$O_6$ as a pentavalent and that the compound is only stable in a reducing atmosphere at high temperature.

**Acknowledgement.** This research was supported by the Korean Ministry of Education in 1988.

## References

1. F. Galsso and J. Pyle, *Inorg. Chem.*, **2**, 482 (1963).
2. E. W. Kaleveld, D. J. Bruntinck, J. P. Dotman and G. Blasse, *J. Inorg. Nucl. Chem.*,**35**, 3928 (1973).
3. A. W. Sleight and J. F. Weiher, *J. Phys. Chem. Solids*, **33**, 679 (1972).
4. J. H. Choy, S. T. Hong and H. M. Suh, *Bull. Kor. Chem. Soc.*, **9**, 345 (1988).
5. M. Walewski, B. Buffat, G. Demazeau, F. Wagner, M. Pouchard and P. Hagenmuler, *Mat. Res. Bull.*,**18**, 881 (1973).
6. M. Walewski, Thesis, Univ. Bordeaux I (1982).
7. J. B. Goodenough, "Magnetism and the chemical bond", Interscience (1963).
8. *NBS circular 539*, **7**, 7 (1957).
9. J. H. Choy and S. T. Hong, *J. Solid State Chem.*, in press (1988).

10. I. Fernandez, R. Greatrex and N. N. Greenwood, *J. Solid State Chem.*, **32**, 97 (1980).
11. T. Nakamura and Y. Gohshi, *Chem. Lett.*, **17 1** (1975).
12. T. Nakamura and J. H. Choy, *J. Solid State Chem.*, **20**, 233 (1977).
13. R. D. Shannon, *Acta Cryst.*, **A32**, 751 (1976).
14. G. Blasse and A. F. Corsmit, *J. Solid State Chem.*, **6**, 513 (1973).
15. A. F. Corsmit, H. E. Hoefdraad and G. Blasse, *J. Inorg. Nucl. Chem.*, **34**, 3401 (1972).
16. N. Ramadas, J. Gopalaskrishanan and M. V. C. Sastri, *J. Inorg. Nucl. Chem.*, **40**, 1453 (1978).
17. J. T. Last, *Phys. Rev.*, **105**, 1740 (1957).
18. P. W. Selwood, "Magnetochemistry" 2nd ed., chap. 5, Interscience, New York (1956).
19. B. D. Cullity, "Elements of X-ray diffraction" 2nd ed., p. 139, Addision-Wesley (1978).

# Reduction of Tertiary Amides with Borane in the Presence of Trimethyl Borate

**In Hwan Oh and Nung Min Yoon***

*Department of Chemistry, Sogang University, Seoul 121-742*

**Young Soo Gyoung**

*Department of Chemistry, Kangreung National University, Kangreung 210-320.* *Received July, 1, 1988*

Various tertiary amides have been subjected to the reduction by borane-THF in the presence of trimethyl borate at 0 °C and the product ratio of alcohol and amine have been analyzed in order to find out the possible way to obtain one product exclusively on the basis of the structure of amides. In the case of N,N-dimethyl derivatives of both linear aliphatic and aromatic amides the corresponding alcohols were produced predominantly. However, the bulkier tertiary amides such as N,N-diethyl and hindered acid derivatives afforded amines rather than alcohols. The mechanism of borane reduction of tertiary amides is also discussed.

## Introduction

The reduction of tertiary amides with various metal hydrides such as lithium aluminum hydride, aluminum hydride, diborane, etc.[1] generally proceeds with carbon-oxygen fission to give the corresponding tertiary amines. Borane-dimethyl sulfide has also been shown to be an excellent selective reducing agent for the reduction of tertiary amides to the corresponding amines.[2] On the other hand, the reduction of tertiary amides to the corresponding alcohols is reported only with $LiEt_3BH$[3], 9-BBN[4] and sodium dimethylaminoborohydride[5]. However, $LiEt_3BH$ is a very powerful reducing agent and many functional groups may not be expected to tolerate this strong hydride. 9-BBN was also reported to give 80% yield of benzyl alcohol from N,N-dimethylbenzamide; however no data is available for the aliphatic tertiary amides. Although sodium dimethylaminoborohydride seems to be a good reagent, it requires a long reaction time at elevated temperature (5-55 h at 66 °C) for such reaction. Recently, we have observed an unexpected high ratio of 1-hexanol over N,N-dimethylhexylamine (ca. 9:1) in the competitive reaction of N,N-dimethylhexanamide and butylene oxide with $BH_3$-$NaBH_4$ system at 0 °C in 1 h.[6] This suggests the alkoxyborane, formed during reaction, might play an important role for the rate enhancement and for the product ratio in the reduction of tertiary amides. Therefore we have decided to explore in detail the reduction of tertiary amides with borane-THF in the presence of trimethyl borate as a catalyst.

## Results and Discussion

**Effect of Temperature.** In order to understand the influence of temperature on the reduction of amides, N,N-dimethylhexanamide and N,N-dimethylbenzamide were subjected to the reduction with borane at 65 °C, 25 °C and 0 °C, respectively, and the results are summarized in Table 1. As shown in Table 1, we can see the temperature effect on the formation of products. Generally, the yields of amines increase with increasing reaction temperature and on the contrary the yields of alcohols increase with lowering temperature. Thus, at 65 °C both amides were reduced to the corresponding tertiary amines almost exclusively; however, the yield of alcohol was increased with lowering temperature. In the case of reaction at 0 °C, N,N-dimethylhexanamide and N,N-dimethylbenzamide gave the corresponding alcohols and aldehydes as major products (66-90%) along with the corresponding amines (34-8%). At 25 °C, we found the amount of tertiary amines increased continually with time at the expense of alcohols and aldehydes. Thus, N,N-dimethylhexylamine increased from 35% (1 h) to 78% (6 h) and the amount of alcohol and/or aldehyde decreased from 65% (1 h) to 22% (6 h). The reduction of tertiary amides is generally believed to proceed along two pathways to afford either amines by reductive removal of carbonyl (path A) or alcohols *via* expulsion of amine and reduction of the resulting aldehyde (path B), through the tetrahedral intermediate I.[1b]

According to this scheme, our results indicate that (1) the